RSC Advances

ROYAL SOCIETY OF CHEMISTRY

www.rsc.org/advances

RSC Advances

ARTICLE

Following the Thermal and Chemical Activation of Supported Au Clusters using X-ray Absorption Spectroscopy

Received 00th January 20xx,
Accepted 00th January 20xx

DOI: 10.1039/x0xx00000x

www.rsc.org/

A. Shivhare,[a] R. W. J. Scott[a]*

Al_2O_3-supported $Au_{25}(SC_8H_9)_{18}$ clusters with various Au loadings were thermally and chemically treated in order to determine the most efficient method towards the removal of thiolate stabilizers while avoiding unwanted increases in cluster size due to agglomeration and sintering. X-ray absorption spectroscopy (XAS) and transmission electron microscopy (TEM) were used to investigate samples before and after thermal and chemical treatments. Results show that while 250°C thermal treatment leads to nearly complete removal of thiolate stabilizers, it comes with a concomitant increase in cluster size as sintering becomes problematic. In contrast, chemical reduction treatments using borohydride reducing agents does not lead to significant growth in cluster size, but only allows for partial thiolate removal. These results are important as many researchers look to determine optimal activation conditions for ultra-monodisperse Au and bimetallic clusters for use as model catalysts without destroying their original structures.

Introduction

Au clusters, owing to their stability and well-defined structures, have recently emerged as an important class of materials in order to study the size and structure related properties of Au nanocatalysts.[1-3] Among all existing Au clusters, $Au_{25}(SR)_{18}$ clusters have gained special attention due to their high yield synthesis and exceptional stability.[4-6] Recently, several research groups have shown that $Au_{25}(SR)_{18}$ clusters in solution and on various support materials can act as catalysts for a variety of catalytic reactions such as CO oxidation, hydrogenation of nitrobenzene and its derivatives, styrene oxidation, semi-hydrogenation of terminal alkynes, and alcohol oxidations.[7-13] In many of these studies, the catalytic activity of Au clusters has been found to be affected by the steric bulk of the thiolate stabilizers, and a positive effect on the catalytic activity was found upon removal of the stabilizers. Removal of thiolate stabilizers has been mostly carried out by calcining these clusters at moderate temperatures, which leads to the partial or complete removal of thiolate stabilizers. For example; Tsukuda and coworkers found that thermal activation of porous carbon supported $Au_{25}(SR)_{18}$ clusters at 450°C led to an enhancement in the catalytic activity and selectivity for benzyl alcohol oxidation.[7] Wu *et al.* found that CeO_2-supported Au_{25} clusters can be activated for CO oxidation catalysis by partially removing thiolate stabilizers at 150°C.[11] Our group reported that mesoporous carbon-supported Au_{25} clusters can be thermally activated for p-nitrophenol reduction catalysis by removing thiolate stabilizers at temperatures as low as 125°C.[10]

While the effect of temperature on the removal of thiolate stabilizers from supported Au_{25} clusters for catalysis has been studied by a number of groups, the effect of chemical reducing agents on the removal of thiolate stabilizers from supported Au clusters has not been studied much. This is despite the presence of literature reports suggesting that borohydride species can reductively desorb thiolate stabilizers from the surface of thiolate-protected Au nanoparticles in solution.[14,15] Recently Asefa and coworkers showed that BH_4^- treatment of supported thiolate-protected Au_{25} and Au_{144} clusters led to an enhancement in the catalytic activity for styrene oxidation and this enhancement was attributed to the partial removal of thiolate stabilizers after BH_4^- treatment.[12]

Herein, we document a detailed investigation of the removal of thiolate stabilizers from supported $Au_{25}(SC_8H_9)_{18}$ clusters with various Au loadings using thermal and chemical strategies using X-ray Absorption Spectroscopy (XAS) and TEM particle size analyses. Thermal treatment of supported $Au_{25}(SC_8H_9)_{18}$ clusters at 250°C leads to nearly complete removal of thiolate stabilizers, albeit with a concomitant growth in cluster size. Treatment using various hydride reducing agents; however, did not lead to significant growth in cluster size, but only leads to partial thiolate removal. Our data show that very distinct features in the X-ray absorption near edge (XANES) and extended X-ray absorption fine structure (EXAFS) spectra can be used to follow the thiolate removal process from supported $Au_{25}(SC_8H_9)_{18}$ clusters and associated changes in cluster size during thermal and chemical treatments. To the best of our knowledge, this is the first study showing EXAFS evidence of the removal of thiolate stabilizers

[a]*Department of Chemistry, University of Saskatchewan, 110 Science Place, Saskatoon, SK S7N 5C9, Canada, E-mail: robert.scott@usask.ca; Tel:1-306-966-2017.*

[†]*Electronic Supplementary Information (ESI) available: XANES and EXAFS fitting data for 2.5% wt samples. See DOI: 10.1039/x0xx00000x*

from supported $Au_{25}(SC_8H_9)_{18}$ clusters using borohydride reducing agents.

Experimental

Hydrogen tetrachloroaurate(III) trihydrate ($HAuCl_4 \cdot 3H_2O$, 99.9% on metal basis, Alfa Aesar), tetraoctylammonium bromide (TOAB, 98%, Aldrich), phenylethanethiol (C_8H_9SH, 99%, Acros Organics), sodium borohydride ($NaBH_4$, 98%, EMD), and aluminum oxide (Al_2O_3, 58Å, ~150 mesh) were used as received. High purity acetonitrile was purchased from Fischer Scientific. High purity tetrahydrofuran was purchased from EMD and 100% ethanol was purchased from Commercial Alcohols. 18 MΩ cm Milli-Q (Millipore, Bedford, MA) deionized water was used throughout.

Synthesis of $Au_{25}(SC_8H_9)_{18}$ clusters

Synthesis of $Au_{25}(SC_8H_9)_{18}$ clusters is reported elsewhere [4]. Briefly, 500 mg of $HAuCl_4 \cdot 3H_2O$ in 50 mL of THF was mixed with 1.2 equiv. of TOAB. To this solution, 5 equiv. of phenylethanethiol was added dropwise and the mixture was left for stirring till it became clear. Subsequently, 10 equiv. of $NaBH_4$ in 10 mL of ice cold water was added all at once. Resulting solution was stirred for four days. After four days, the reaction was stopped and the solvent was evaporated completely. The resulting solid was then washed with a mixture of ethanol/water several times to remove excess leftover thiol and disulfide species, and finally the residue was dried using a rotary evaporator. The resulting $Au_{25}(SC_8H_9)_{18}$ clusters were extracted with acetonitrile.

Synthesis of Al_2O_3-supported $Au_{25}(SC_8H_9)_{18}$ clusters

Supported clusters were prepared by immobilizing the required amount on $Au_{25}(SC_8H_9)_{18}$ clusters dissolved in THF on 200 mg of Al_2O_3 support using a wetness impregnation approach, and the obtained solid was dried by purging the sample using N_2 gas. As prepared supported clusters were stored under at 0°C under inert atmosphere prior to TEM and EXAFS analysis.

Thermal and hydride treatment

200 mg of supported $Au_{25}(SC_8H_9)_{18}$ clusters with different metal loadings were treated at 250°C under air atmosphere for 90 minutes. Treatment with $LiAlH_4$ and $LiBH_4$ was carried out by suspending 100 mg of supported samples in 5mL of hexane, followed by the addition of 70 equiv. of $LiAlH_4$ and $LiBH_4$ with respect to $Au_{25}(SC_8H_9)_{18}$ clusters. These solutions were stirred for 10 minutes and subsequently washed with hexane and water. Treatment with $NaBH_4$ was carried out by first mixing 100 mg of supported samples and 3500 equiv. of $NaBH_4$ with respect to $Au_{25}(SC_8H_9)_{18}$ clusters. To this mixture was then added 5 mL of deionized water and resulting mixture was allowed to stir for 20 minutes. After that, the resulting solid was washed with plenty of water and dried under vacuum.

Characterization Methods

Transmission electron micrographs (TEM) were taken with a HT7700 TEM operating at 100 kV. TEM grids were prepared by placing a drop of sample suspended in hexane on graphene-enhanced lacey carbon TEM grids (Electron Microscopy Sciences). 20-30 particles were analyzed in order to calculate the average size and standard deviation. All samples used for EXAFS analysis were prepared by supporting phenylethanethiol-protected Au_{25} clusters with different loadings, 2.5%, 1.5%, 0.75%, and 0.2% by metal weight on an Al_2O_3 support (58 Å, ~150 mesh) using a wetness impregnation approach. EXAFS measurements were conducted at the Hard X-ray MicroAnalysis (HXMA) beamline 061D-1 (energy range 5–30 keV; resolution, 1×10^{-4} ΔE/E) of the Canadian Light Source (CLS, 2.9 GeV storage ring, 250 mA current). Samples was pressed into pellets and measured in transmission (2.5% and 1.5% loadings by metal weight) and fluorescence (0.75 and 0.2% loadings by metal weight) modes by measuring the Au L_3-edge. A double-crystal Si (111) was employed for energy selection. Higher harmonics were eliminated by detuning double-crystal using a Rh coated KB mirrors for the Au L_3-edge. The incident and transmission X-ray intensities were detected by ion chambers filled with helium–nitrogen mixtures for transmission measurements, and a 32 element detector was used for fluorescence measurements. The IFEFFIT software package was used for data processing.[16] For the data analysis, the amplitude reduction factor, S_0^2, was found from fitting Au foil and subsequently fixed at 0.90. For EXAFS data fitting, a standard $Au_{25}L_{18}$ crystal structure was using in order to fit the as-synthesized, $LiAlH_4$ and $LiBH_4$ treated samples.[10] Au face centered cubic (fcc) and AuS models were used to fit thermally-treated and $NaBH_4$-treated samples.

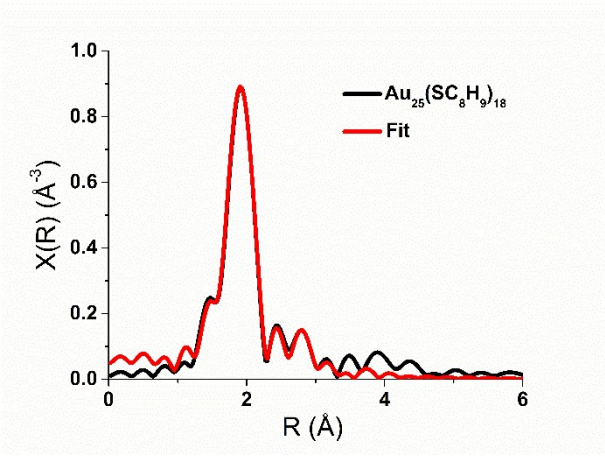

Figure 1. EXAFS fitting in R-space of Al_2O_3-supported $Au_{25}(SC_8H_9)_{18}$ clusters with 2.5% loading by metal weight.

Results and discussion

Figure 1 shows the EXAFS fitting in *R*-space of Al_2O_3-supported $Au_{25}(SC_8H_9)_{18}$ clusters with 2.5% loading by Au weight in *R*-space. The data shows one major peak at *ca*. 2 Å due to the scattering of photoelectrons from neighboring sulphur atoms along with three much smaller Au-Au peaks (~ 2.2-3.2 Å), which have been shown by Zhang and coworkers to be due to different Au-Au bonding pairs present within Au_{25}

Table 1. EXAFS fitting parameters of Al_2O_3-supported $Au_{25}(SC_8H_9)_{18}$ clusters with 2.5% loading by metal weight.

	CN	R (Å)	σ^2 (Å^2)	Eo (eV)
Au-S	1.4(1)	2.313(5)	0.001(4)	2.2 (7)
Au-Au(core, 1)	1.44[1]	2.732(4)	0.007(1)	6.2 (1.2)
Au-Au (surface, 2)	1.92[1]	2.94(5)	0.016(5)	6.2 (1.2)
Au-Au (staple, 3)	2.88[1]	3.30(8)	0.04(2)	6.2 (1.2)

[1]Au-Au coordination numbers were fixed as discussed in ref [10, 17]

clusters.[10,17] The first Au-Au (core) peak is due to the bonding between the central Au atom of the icosahedron core of the clusters and 12neighboring Au atoms along with six short Au-Au pairs present on Au_{13} surface with an average Au-Au bond distance of 2.73 Å (designated Au-Au core contribution). The second Au-Au peak is due to the presence of larger Au-Au pairs on the surface of Au_{13} core with the Au-Au bond distance of 2.94 Å and is given the designation Au-Au surface contribution. The last Au-Au (staple) peak is due to the bonding between Au atoms from staple motifs and Au atoms from the surface of the Au_{13} core with the Au-Au distance of 3.3 Å.[17] Due to the phase shift of the exited photoelectron, Au-Au bonding pairs in *R*-space data (Figure 1) are at lower R values compared to the bond distance values obtained from single crystal data.[18] In order to fit the EXAFS data, different Au-Au coordination numbers were fixed to that obtained from the literature crystal structures and the rest of the parameters were allowed to vary (Table 1). Here, interestingly, we found that the Au-S coordination number value of 1.4 (1) was lower than the value reported for intact $Au_{25}(SR)_{18}$ clusters by both ourselves and others (Au-S, CN = 2.0).[10,17] This is a very interesting finding and we attribute it to the partial removal of thiolate groups after the immobilization of $Au_{25}(SC_8H_9)_{18}$ clusters on the oxide support.

Recently, various groups have reported that oxide supported $Au_{25}(SR)_{18}$ clusters show catalytic activity at moderate temperature without any high temperature thermal activation.[19-21] This finding provides a possible explanation to this by attributing the catalytic activity of these supported clusters to a decrease in Au-S coordination number, which opens up the active sites for catalysis. Figure 2 shows the EXAFS data in R-space of Al_2O_3 supported $Au_{25}(SC_8H_9)_{18}$ clusters with 1.5% loading by Au weight after thermal (250°C) and chemical treatments. BH_4^- and thermal treatments led to a decrease in the Au-S contribution and increase in the Au-Au contribution. The decrease in the Au-S contribution shows removal of thiolate stabilizers from the surface of Au clusters, and the increase in the Au-Au contribution shows growth in cluster size. EXAFS fittings in *R*-space after thermal and chemical treatment is shown in Figure 3. Full fitting parameters for each of the samples are found in Table 2.

Data show that the Au-S contribution below 2 Å decreases in intensity after treatment with different reducing agents and completely disappears after thermal treatment at 250°C. After $LiAlH_4$ treatment, the Au-Au contributions experienced very

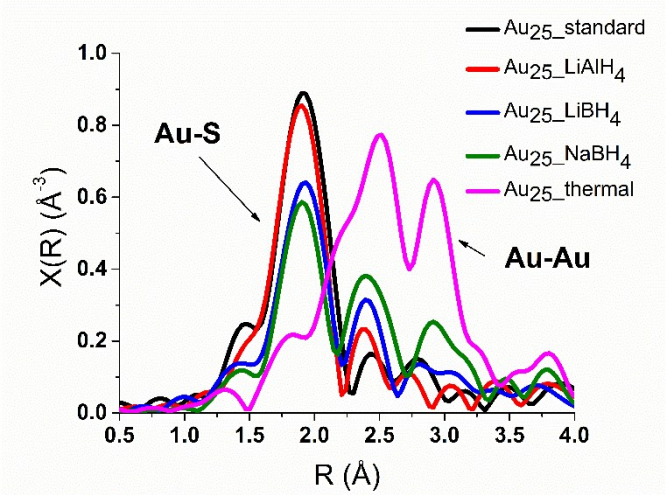

Figure 2. EXAFS data in *R*-space of thermally and chemically treated Al_2O_3-supported $Au_{25}(SC_8H_9)_{18}$ clusters with 1.5% loading by metal weight.

little change; however, significant changes were observed after treatment with $LiBH_4$ and $NaBH_4$. After $LiBH_4$ treatment, the Au-Au staple (Au-Au 3) contribution could not be fit, which is likely due to the fact that BH_4^- reducing agent reacted with the thiolate stabilizers present in these staple motifs. This is evident by the decrease in Au-S coordination number from 1.4 (1) in the case of Al_2O_3-supported $Au_{25}(SC_8H_9)_{18}$ clusters to 0.8 (1) after $LiBH_4$ treatment. Treatment of Al_2O_3-supported $Au_{25}(SC_8H_9)_{18}$ clusters with $NaBH_4$ led to significant changes in both the Au-S and Au-Au coordination number values, such that only one Au-Au first shell fcc contribution could be fit. The Au-S coordination number decreased to 0.6 (1) and the Au-Au coordination number was found to be 6.1 (7). The low Au-Au coordination number value after $NaBH_4$ treatment (6.1 ± 0.7) compared to thermal treatment (9.7 ± 0.5) shows very little growth in cluster size after $NaBH_4$ treatment. The correlation between coordination numbers obtained from EXAFS analysis and particle size (calculated theoretically using imperial formulae) suggests that cluster size changes from 25 Au atoms to *ca.* 30-40 Au atoms after $NaBH_4$ treatment; however, after

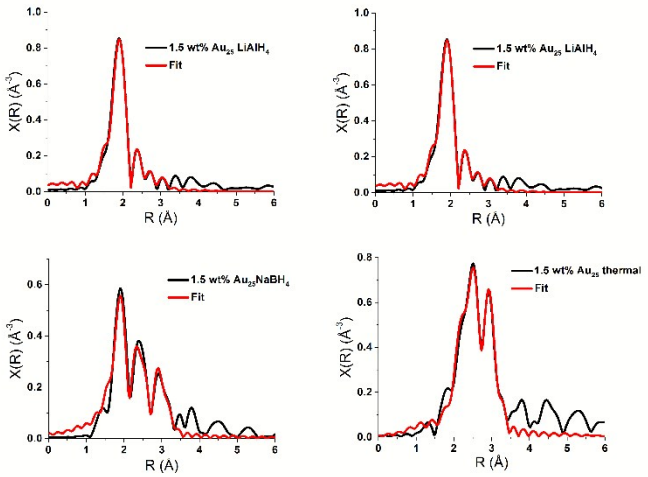

Figure 3. EXAFS fitting in *R*-space of thermally and chemically treated Al_2O_3-supported $Au_{25}(SC_8H_9)_{18}$ clusters with 1.5% loading by metal weight.

Table 2. EXAFS fitting parameters of thermally and chemically treated Al_2O_3-supported $Au_{25}(SC_8H_9)_{18}$ clusters with 1.5% loading by metal weight

		CN	R (Å)	σ^2 (Å^2)	Eo (eV)
$LiAlH_4$	Au-S	1.2 (1)	2.30 (2)	.0007 (8)	-1.1 (1.1)
	Au-Au(1)	1.44[1]	2.73 (2)	.007 (3)	2.2 (3.2)
	Au-Au (2)	1.92[1]	2.89 (3)	.012 (5)	2.2 (3.2)
	Au-Au (3)	2.88[1]	3.2 (1)	.05 (4)	2.2 (3.2)
$LiBH_4$	Au-S	0.8 (1)	2.319 (8)	.0004 (9)	1.0 (1.5)
	Au-Au (1)	1.44[1]	2.7 (3)	.007 (2)	0.8 (1.4)
	Au-Au (2)	1.92[1]	2.85 (4)	.019 (8)	0.8 (1.4)
$NaBH_4$	Au-S	0.6 (1)	2.301 (7)	.001	4.2 (7)
	Au-Au	6.1 (7)	2.83 (1)	.003 (1)	4.2 (7)
250°C Thermal	Au-Au	9.7 (5)	2.846 (4)	.0095 (5)	4.9 (3)

[1]Au-Au coordination numbers were fixed as discussed in ref [10, 17]

thermal treatment cluster size changes to *ca.* 400 Au atoms.[10] It is important to note that the $NaBH_4$ studies were done at much higher concentrations than $LiBH_4$/$LiAlH_4$ studies in order to try to attempt to fully remove thiol stabilizers, and thus differences between $LiBH_4$ and $NaBH_4$ are likely mostly due to higher concentrations of $NaBH_4$ used. We have also analyzed EXAFS data in *R*-space for Al_2O_3-supported $Au_{25}(SC_8H_9)_{18}$ clusters with 2.5% loading by metal weight (see ESI), and data shows similar trends to the 1.5% by weight sample data.

TEM analysis (Figure 4) of the Al_2O_3-supported $Au_{25}(SC_8H_9)_{18}$ clusters was also carried out. The initial clusters are hard to discriminate from the Al_2O_3 support, but those measured have an average size of 1.0 ± 0.2 nm, which is consistent with their expected size. After thermal treatment at 250°C, the clusters grew to 1.8 ± 0.4 nm, while BH_4^- treatment led to a final size of 1.3 ± 0.3 nm. TEM data show that while thermal treatment leads to significant growth in cluster size, borohydride treatments leads to almost negligible growth in size, which further corroborates our previous EXAFS findings. Correlation of first-shell coordination number values obtained by EXAFS after thermal and $NaBH_4$ treatments with number of Au atoms obtained theoretically suggest that after $NaBH_4$ treatment, the cluster size grew from 25 Au atoms to ~30-40 Au atoms, and after thermal treatment, the number of Au atoms in the clusters grows significantly to *ca.* 450 Au atoms.[10]

Figure 5 shows the Au-L_3 XANES data of Al_2O_3-supported $Au_{25}(SC_8H_9)_{18}$ clusters with 1.5% loading by Au weight before and after thermal and chemical treatments. The inset shows the XANES edges for each of the samples. While there are only minimal differences at the white line (at *ca.* 11930 eV) suggesting no change in oxidation state, a clear trend can be seen beyond the white-line region (marked peaks), with a new peak growing at *ca.* 11950 eV as the clusters show greater thiolate removal. Comparing this data with the Fourier transformed EXAFS data in *R*-space (Figure 3) suggests that these new features are related to the decrease in Au-S contribution and increase in Au-Au contribution, and thus

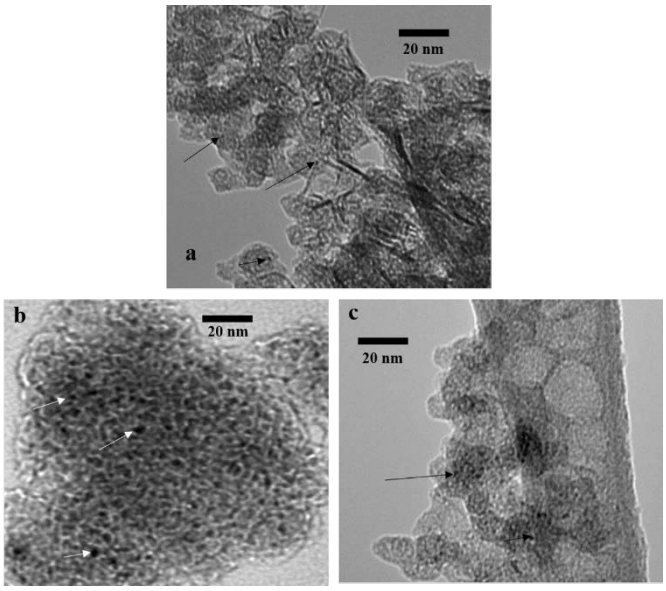

Figure 4. TEM images of a) as synthesized $Au_{25}(SC_8H_9)_{18}$ clusters with 1.5% loading by metal weight, b) thermally treated $Au_{25}(SC_8H_9)_{18}$ clusters with 1.5% loading by metal weight, and c) $NaBH_4$ treated $Au_{25}(SC_8H_9)_{18}$ clusters with 1.5% loading by metal weight.

increase in cluster size. We believe this 11950 eV peak is a multi-scattering peak, such that its' intensity is related to the number of shells around absorbing atoms; small Au clusters which do not have many upper-shell Au neighbours thus show a much lowered intensity.

The generality of these features was established by analyzing XANES data at various Au loadings (see ESI); similar trends in the XANES were observed for various Au loadings. This is important as it shows that XANES, as well, can be used to study small changes in the cluster size and structure during thiolate removal, which is sometimes very difficult to study with EXAFS data alone due to the poor quality of data at low Au loadings.[11]

It has been reported in the literature that desorption of two-dimensional thiolate self-assembled monolayers from Au surfaces takes place at a potential of *ca*. 1.0 V to -1.3 V (*vs*. NHE). $NaBH_4$ has a standard oxidation potential of 1.24 V vs. NHE in basic conditions, and therefore can desorb thiolate monolayers from Au surface.[22] For a planar Au surface covered with two-dimensional self-assembled thiolate monolayers, dissociation mechanism is rather simple and involves the reductive desorption of organic thiolates via one electron transfer.[23] However, in the case of $Au_{25}(SR)_{18}$ clusters, due to the presence of two spatially different thiolates in staple motifs, the exact determination of the point of cleavage is not clear. Asefa and coworkers have reported that thiolate desorption from $Au_{25}(SR)_{18}$ clusters occurs at a negative potential of *ca*. -1.5 V; however, no comment was made on the selectivity of thiolate removal.[12] Jin and coworkers showed using NMR spectroscopy that in the case of glutathione protected Au_{25} clusters, thiolates bonded with only staple Au atoms are more vulnerable to attack by $Ce(SO_4)_2$ than thiolates bonded with the Au_{13} core directly.[24] In our study, in the case of $LiBH_4$ treatment suggests that Au_{13} core was completely preserved, as we were able to fit EXAFS data after fixing Au-Au (core) and Au-Au (surface) coordination numbers

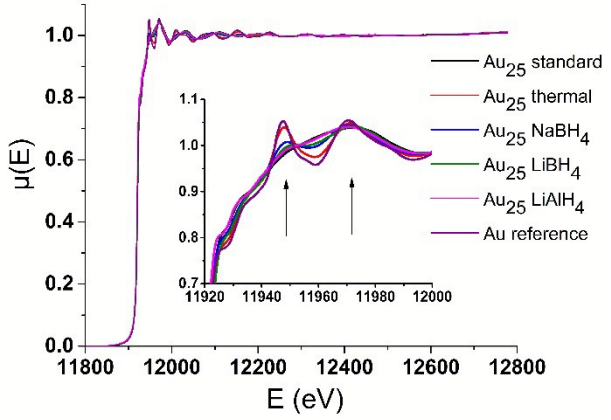

Figure 5. XANES data of thermally and chemically treated Al_2O_3-supported $Au_{25}(SC_8H_9)_{18}$ clusters with 1.5 % loading by metal weight.

representative of Au_{13} core. However, the inability to fit Au-Au (staple) contributions suggests that BH_4^- was perhaps reducing weaker thiolates bonded with only staple Au atoms. After $NaBH_4$ treatment, both types of thiolates were found to be mostly desorbed as the increase in Au-Au coordination number value due to the growth in cluster size was observed. In our previous study, we showed that $Au_{25}(SR)_{18}$ clusters were relatively more stable towards $NaBH_4$ in solution than their larger counterparts.[25] The present study however suggests that oxide supported $Au_{25}(SR)_{18}$ clusters are less stable towards $NaBH_4$ than the same clusters in solution, as some thiols are removed upon absorption onto the oxide support. Our data also suggests that by varying the amount and the strength of the reducing agents, one can partially remove the thiolate stabilizers under relatively mild conditions (chemical treatments). This result shows promise towards developing strategies that allow for selectively accessing active sites for catalysis.

Conclusions

In summary, we have shown that thiolate stabilizers can be removed partially from oxide-supported $Au_{25}(SR)_{18}$ clusters under milder conditions (using borohydride reducing agents) with particle sizes much smaller than that seen under harsher temperature treatments (250°C thermal treatment). TEM data suggest that thermal treatment leads to significant growth in cluster size; however, borohydride treatment leads to almost negligible growth in size during thiolate removal. EXAFS data suggests that partial desorption of thiolate stabilizers was observed after the immobilization of these clusters on oxide supports. This is an important finding, as it can help explain the catalytic activity of oxide supported $Au_{25}(SR)_{18}$ clusters before any thermal activation step. Finally we have shown that very distinct features in the XANES region can be used to follow this thiolate removal process and the concomitant growth in cluster size. This is particularly important in the case of low Au loadings, where it becomes very difficult to obtain high-quality EXAFS data.

Acknowledgements

The authors acknowledge financial assistance from the National Sciences and Engineering Research Council of Canada (NSERC) and thank Ning Chen and Weifeng Chen at the Canadian Light Source for assistance with XAS measurements. EXAFS experiments described in this paper were performed at the Canadian Light Source, which is supported by the Natural Sciences and Engineering Research Council of Canada, the National Research Council Canada, the Canadian Institutes of Health Research, the Province of Saskatchewan, Western Economic Diversification Canada, and the University of Saskatchewan.

Notes and references

1 G. Li, D. E. Jiang, S. Kumar, Y. X. Chen and R. Jin, *ACS Catal.,* 2014, **4**, 2463-2469.
2 K. G. Stamplecoskie and P. V. Kamat, *J. Am. Chem. Soc.,* 2014, **136**, 11093-11099.
3 Y. Zhu, H. F. Qian, A. Das and R. Jin, *Chinese J. Catal.*, 2011, **32**, 1149-1155.
4 A. Shivhare, S. J. Ambrose, H. X. Zhang, R. W. Purves and R. W. J. Scott, *Chem. Commun.*, 2013, **49**, 276-278.
5 Y. Shichibu, Y. Negishi, H. Tsunoyama, M. Kanehara, T. Teranishi and T. Tsukuda, *Small*, 2007, **3**, 835-839.
6 M. A. Tofanelli and C. J. Ackerson, *J. Am. Chem. Soc.*, 2012, **134**, 16937-16940.
7 T. Yoskamtorn, S. Yamazoe, R. Takahata, J. Nishigaki, A. Thivasasith, J. Limtrakul and T. Tsukuda, *ACS Catal.*, 2014, **4**, 3696-3700.
8 J. Fang, J. G. Li, B. Zhang, X. Yuan, H. Asakura, T. Tanaka, K. Teramura, J. P. Xie and N. Yan, *Nanoscale*, 2015, **7**, 6325-6333.
9 Y. M. Liu, H. Tsunoyama, T. Akita and T. Tsukuda, *Chem. Commun.*, 2010, **46**, 550-552.
10 A. Shivhare, D. M. Chevrier, R. W. Purves and R. W. J. Scott, *J. Phys. Chem. C*, 2013, **117**, 20007-20016.
11 Z. Wu, D-E. Jiang, A. K. P. Mann, D. R. Mullins, Z-A. Qiao, L. F. Allard, C. Zeng, R. Jin and S. H. Overbury, *J. Am. Chem. Soc.*, 2014, **136**, 6111-6122.
12 S. Das, A. Goswami, M. Hesari, J. F. Al-Sharab, E. Mikmekova, F. Maran, and T. Asefa *Small*, 2014, **10**, 1473-1478.
13 G. Li, and R. Jin *J. Am. Chem. Soc.*, 2014, **136**, 11347-11354.
14 D. F. Yang, C. P. Wilde and M. Morin, *Langmuir*, 1996, **12**, 6570-6577.
15 S. M. Ansar, F. S. Arneer, W. F. Hu, S. L. Zou, C. U. Pittman and D. M. Zhang, *Nano Lett.*, 2013, **13**, 1226-1229.
16 M. Newville, B. I. Boyanov and D. E. Sayers, *J. Synchrotron Rad.*, 1996, **6**, 264-265.
17 M. A. MacDonald, D. M. Chevrier and P. Zhang, *J. Phys. Chem. C*, 2011, **115**, 15282-15287.
18 A. Gaur, B. D. Shrivastava and H. L. Nigam, *Proc. Indian. Nat. Sci. Acad*. 2013, 921-966.
19 Y. Zhu, H. F. Qian, B. A. Drake and R. Jin, *Angew. Chem., Int. Edit.,* 2010, **49**, 1295-1298.
20 X. T. Nie, H. F. Qian, Q. J. Ge, H. Y. Xu and R. Jin, *ACS Nano*, 2012, **6**, 6014-6022.
21 J. Liu, K.S. Krishna, Y. B. Losovyj, S. Chattopadhyay, N. Lozova, J. T. Miller, J. J. Spivey and S. S. R. Kumar, *Chem-Eur. J.*, 2013, **19**, 10201-10208.
22 C. A. Widrig, C. Chung and M. D. Porter, *J. Electroanal. Chem.*, 1991, **310**, 335-359.
23 B. M. Quinn and K. Kontturi, *J. Am. Chem. Soc.*, 2004, **126**, 7168-7169.

24 Z. Wu, C. Gayathri, R. R. Gil and R. Jin, *J. Am. Chem. Soc.*, 2009, **131**, 6535-6542.
25 M. Dasog, W. Hou, and R. W. J. Scott, *Chem. Commun.*, 2011, **47**, 8569-8571.

Graphical Abstract

X-ray absorption spectroscopy has been used to follow a mild chemical route using $NaBH_4$ reducing agent for the activation of atomically-precise Au clusters for catalysis.